



Contents lists available at **CEPM**

Journal of Computational Engineering and Physical Modeling

Journal homepage: <http://www.jcepm.com/>



## Numerical Simulation of Concrete Mix Structure and Detection of its Elastic Stiffness

**M. Mahdi<sup>1</sup> and I. Marie<sup>2\*</sup>**

1. Department of Mechanical Engineering, College of Engineering, King Faisal University, Al Hofoof, KSA

2. Department of Civil Engineering, Faculty of Engineering, Hashemite University, Zarqa, Jordan

Corresponding author: [iqbal@hu.edu.jo](mailto:iqbal@hu.edu.jo)



<http://dx.doi.org/10.22115/cepm.2018.54011>

### ARTICLE INFO

#### Article history:

Received: 13 November 2017

Revised: 14 December 2017

Accepted: 16 December 2017

#### Keywords:

Mechanical properties,

Stiffness,

2-D Finite element analysis (FEA),

Concrete Mix.

### ABSTRACT

Concrete mix stiffness (CM) primarily relies on its ingredients, which mainly consists of stone aggregate and mortar. To analyse the role of the components of CM on its properties a numerical simulation of CM structure is conducted. Within the scope of this study, the structure and the properties of CM are simulated using ANSYS code to apply the finite element method (FEM). The size of aggregate is modelled using direct random nodes and elements and the problem is approximated as two-dimensional plane one. Different ratios of aggregate and mortar were considered to determine their influence on the stiffness of CM. The CM is treated as bi-composite and subjected to compressive loading. For determining the influence of the proportion of stone aggregate on the stiffness of CM, the used specimens only differ in the amount of stone aggregate and their shapes. Although the stone aggregates are assumed to be of cylindrical shapes (plane conditions), the compressive stiffness of CM works well with the mixture rule.

### List of nomenclatures

CM concrete mix

$E_{CM}$  Elastic stiffness of concrete mix



p	volume proportion of stone aggregate in concrete mix
$R_s$	ratio of stone aggregate stiffness to that of mortar
r	ratio of reaction force associated with plane stress conditions to that of plane strain ones
SA	stone aggregate
$\nu_{CM}$	Poisson's ratio of concrete mix
$\sigma_C$	average compressive stress of concrete mix

## 1. Introduction

It has been acknowledged that concrete mix structure may be considered as a three-phase composite material, consisting of a coarse aggregate single phase, a cement mortar phase and an interface zone of transition between cement mortar and coarse aggregates (ITZ). Each phase has an impact on the behaviour of concrete. Several experiments have been conducted to examine each phase influence on the mechanical properties of concrete. Persson [1] studied experimentally and numerically some mechanical properties, of self-compacting concrete as well as normal compacting concrete. The nano structural and mechanical properties of concrete samples were discussed by Bahari et al. [2], using atomic force microscopy. Moreover, the mechanical properties of cement mortar and microstructural properties of hardened cement paste were investigated using Fourier Transform Infrared Spectroscopy and X-ray Diffraction [3]. The study of Bahari et al. [4] reveals that the influence of grain boundaries plays strong barriers role to distribution of cracks on the stability of the sample. Wu et al. [5] conducted tests to investigate some mechanical properties of concrete and how they may be affected by the coarse aggregate type. The mechanical properties that studied by Wu et al. [5] are; the compressive strength, fracture energy, splitting tensile strength, and elastic stiffness of concrete having several 28-day target compressive strengths of 30, 60, and 90 MPa. Their results reveal that the compressive and tensile strengths, elastic stiffness, and fracture energy of concrete for a certain water/cement ratio (W/C) rely on aggregate type and properties. Rao & Prasad [6] studied experimentally the behaviour of the interface zone between mortar and aggregate. Additionally, they studied the influence of the aggregate properties, type and roughness, on the bond strength of the IZT to the surface of the aggregates. González-Peña et al. [7] used the electro-optic holographic technique on samples of homogeneous materials to determine its Young's dynamic modulus based on the resonance frequency of the analysed samples and after that they modified the method to account for non-homogeneity in materials such as concrete. Grote et al. [8] conducted experiments to study the dynamic behaviour of concrete and mortar at strain rates of order of  $10^4 \text{ s}^{-1}$  and pressures up to 1.5 MPa. Wong et al. [10] investigated the effect of fly ash on strength and fracture characteristics of the IZT.

Many modelling techniques have been adopted and studies by many researchers. The analytical modelling studies, on the other hand, rely on the structure of concrete. A procedure for generating random aggregate structures was proposed by Wang et al. [10] for aggregate particles of round and angular shapes. Their proposed procedure based on the Monte Carlo random sampling principle. Moreover, they treated the concrete as a three-phase system consisting of three zones; coarse aggregate, mortar medium with fine aggregate immersed in it,

and ITZ between the coarse aggregate and the mortar. Willam et al. [11] examined the behaviour of heterogeneous elastic materials and their stiffness properties. The microstructural features of concrete has been included in the computational studies as a bi-material system composed of aggregate particles which are imbedded in a hardened cement paste taking into account the incompatibility of the two constituents. Lai & Serra [12] developed a model, with sufficient approximation, based on neuro-computing, for predicting the compressive strength of a three phase concrete material. The model was calibrated using a substantial amount of data. Zhao & Chen [13] used a two-dimensional micro-structural model in an analytical solution to obtained the effective elastic moduli of concrete. They studied the relationships between these elastic moduli and that for each constituent of concrete.

Hashin & Monteiro [14] considered concrete mix as a composite materials composed of a mortar matrix with implanted particles of spherical shape. Park et al. [15] used the fully dynamic finite element simulations to analyse concrete and mortar response after applying an impact loading of high-strain-rate taking into consideration the effect of the microstructure of concrete and the load-carrying capacity. Kwan et al. [16] developed a non-linear finite element method suitable for cracking and non-linear constitutive properties of the materials in their mesoscopic study of concrete. Li et al. [17] developed a built-in model of three-layers by considering coarse aggregate particles having spherical shape coated with an ITZ and cement mortar layer with uniform thickness embedded into a corresponding concrete media. To predict the 28 days compressive strength of concrete and recycled aggregate concrete, Khademi et al. [18], [19] used artificial neural network, adaptive neuro-fuzzy inference system, and multiple linear regression as three different data-driven models.

This numerical study focuses on the numerical prediction of the compressive stiffness of concrete mix (CM) using the finite element method by ANSYS code. The CM is treated as bi-composite material subjected to compressive loading. So as to determine the influence of the proportion of stone aggregate on the stiffness of CM, the test samples only differ in the amount of stone aggregate and their shapes.

## **2. Problem model**

### **2.1. Model geometry and material properties**

A cubic specimen of size 150x150x150 mm is considered. The model used in this study represent a plane problem and therefore assumes a plane state of stress or strain. Due to the symmetry of boundary conditions, dividing the specimen into four equal sizes can employ further simplifications and thereby reducing the number of finite elements required for control size modelling. Hence, the symmetry conditions have to be represented by appropriate boundary conditions as shown in Figure 1. The applied compressive load is simulated by a step compressive displacement to induce a compressive strain of 0.001. The effect of friction has been ignored. The computed reaction load is used to estimate the average compressive stress  $\sigma_c$ . By employing plane stress conditions, the elastic stiffness of CM,  $E_{CM}$ , is therefore  $1000 \sigma_c$ . The plane strain model can be built-up through a minor change in the input data of the plane stress

model. The volume percentage of stone aggregate (SA) proportion in CM is represented by  $p$ . To compute the variation of effective Poisson's ratio of concrete mix,  $\nu_{CM}$ , with  $p$ , Hook's law for the assumed plane state of stress and strain conditions were compared. Refereeing to Boresi et al. [20], the ratio,  $r$ , of the reaction load associated with compressive strength of plane stress conditions to that of plane strain ones can be used to estimate  $\nu_{CM}$ , Namely,

$$\nu_{CM} = (1-r)^{1/2} \tag{1}$$

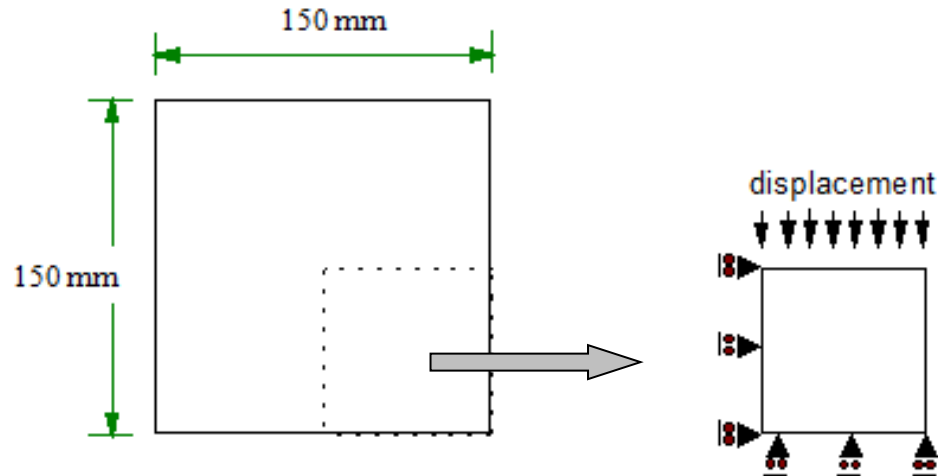


Fig. 1. Problem model.

The compressive stiffness of SA varies between 30 MPa and 45 MPa while that of mortar is 15 MPa. Accordingly, the ratio of stone aggregate stiffness to that of mortar,  $R_s$ , has magnitudes of 2 to 3. Therefore this material model may cover a wide range of CM properties. The modulus of elasticity and Poisson ratio of mortar and SA are shown in Table 1 for different  $R_s$  values.

**Table 1.**  
Mechanical properties of mortar and aggregates.

Property	Mortar	Stone aggregate	
		$R_s = 2$	$R_s = 3$
Modulus of Elasticity	15 MPa	30 MPa	45 MPa
Poisson ratio	0.25	0.3	0.3

## 2.2. Model numerical accuracy

In a non-linear finite element analysis, the variation of solution results with the refinement of the mesh is one of the common tools for accuracy assessment. In this study, the mesh refinement tool is implemented for accuracy assessment as smaller variations in results reflects better solution accuracy.

To estimate the accuracy of the finite element discretization, two styles of mesh generations were employed as fine and coarse meshes. The fine mesh is simply a further division of existing

elements of coarse mesh. This is done by replacing every coarse element by five fine elements with the same area of original coarse element reserved. To refine a coarse element, four intermediate nodes are created such that they are located between coarse element centre and its corners. The resulting fine elements represent a more accurate mesh but at the cost of extra four nodes and four elements for each refined coarse element. Figure 2-a shows a typical coarse element and its associated fine divisions as in Figure 2-b.

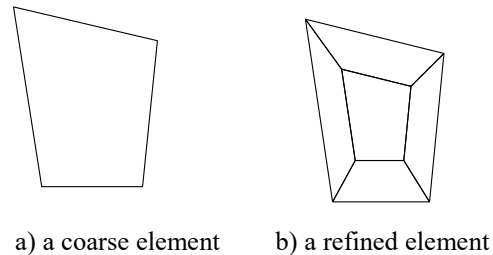


**Fig. 2.** Mesh refinement.

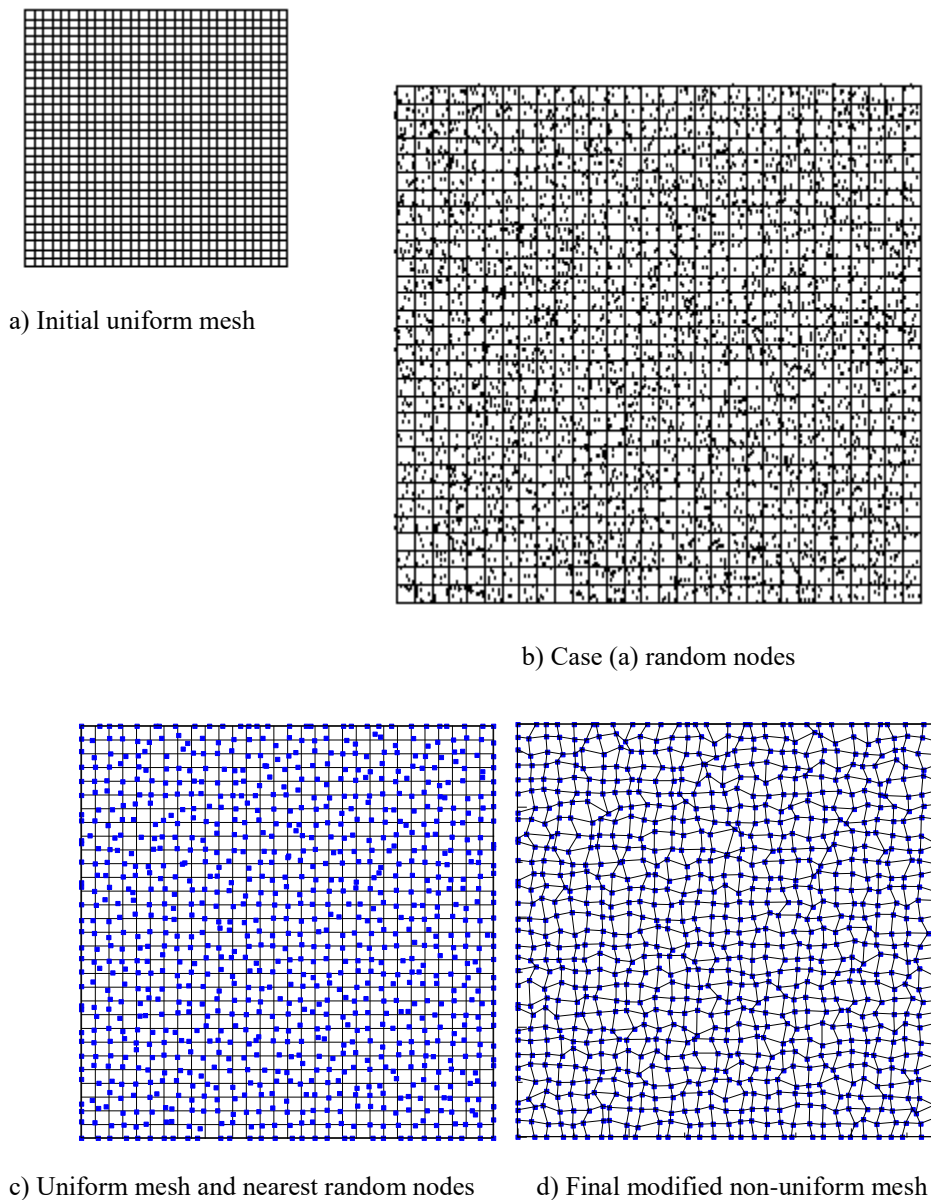
Every case study has an input FEM coarse data generated by a grid of 30x30 elements, which corresponds to 900 elements and 961 nodes. By refining this mesh, the total number of elements and that of nodes are 4500 and 4561 respectively. A typical case study of the uniform mesh may consume a total running time of 40.81 seconds on a computer system rating of 80 MIPS, 20 scalars MFLPOS and 40 vectors MFLOPS.

### 2.3. CM random structure

A Method for randomly generating aggregates of near-rounded shape in a concrete mix structure is illustrated using finite element method. The full random generation of finite element nodes and the assembly of elemental nodes may require an expertise work. Nevertheless, in this study, a simplified procedure is developed. The first step toward a random mesh generation starts with the generation of a uniform mesh of four-noded quadrilateral elements along with their elemental uniform nodes locations UNL. Figure 3-a shows a typical style of nodes and elements. The second step requires a set of new generated random nodes locations RNL to be mapped on the control volume of UNL as in Figure 3-b. The locations of UNL are altered using RNL to produce nearly-random locations of nodes. This is done by a recursive search of the nearest located random node of RNL to a given node in the UNL as in Fig 3-c. Accordingly, the location of an original node of UNL will become the same as that of the nearest random node. The method is repeated for other remaining uniform nodes such that the new location of UNL is adjusted to its new location as in Fig. 3-d. It should be noted that the previous procedure might, in general, produce non-negative jacobian elements, which is a necessary requirement of proper FEM, input data. Accidentally, the alteration of node location may produce erroneous negative-jacobian elements. However, the user-FORTRAN code will discard those elements and produce gaps of zero stiffness, which in turn approximates the presence of air void. The generation of random stone aggregates makes use of similar principle but with circles of random locations and radii. As plane conditions apply, a number of cylinders are used to approximate the three-dimensional shapes of aggregates. The role of random circles (RC) is to enclose those elements, which are to represent stone aggregates. To prevent stone aggregates from touching themselves, an algorithm

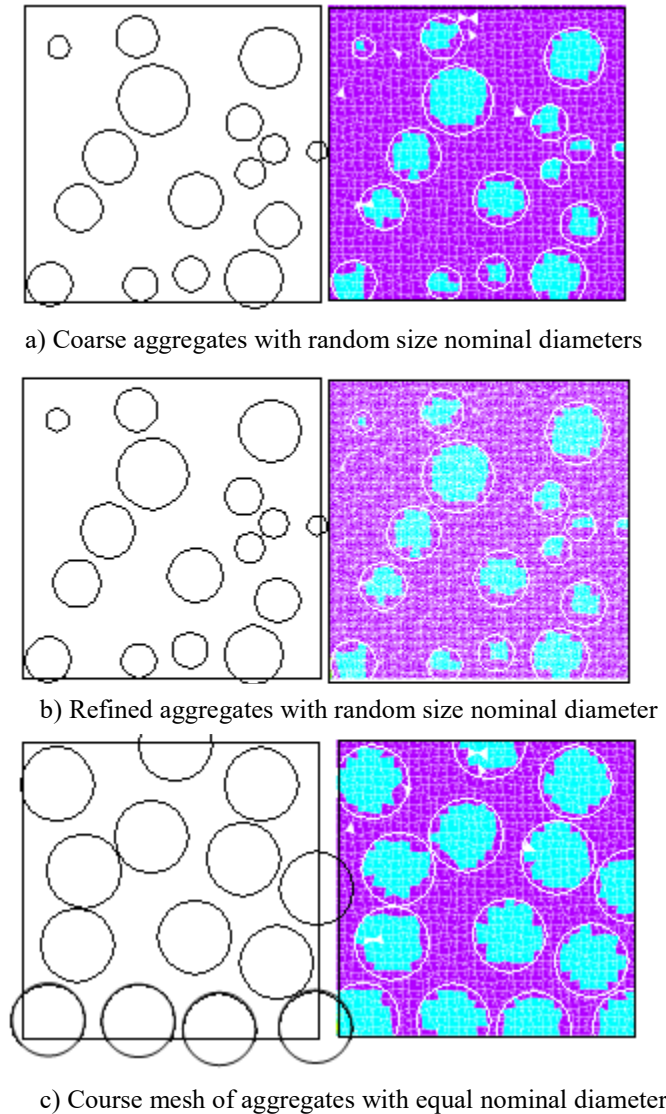
is designed to discard overlapping circles recursively. The rest of elements outside RC represent the mortar. Generally, the shape of stone aggregate may have sharp corners and other shapes, which are investigated, in the second part of this series. It should be noted that the interface between the mortar and stone aggregate is assumed as rigid links. Therefore no cracks are assumed inside the CM structure.

Figure 4 shows typical examples of generated stones aggregates and mortar. It is clear that the selected size of RC and their distribution govern the structure of CM. To control the size of RC, the radius of the circle can be any random value within prescribed tolerance as in Figure 4-a. Figure 4-b shows a refined version of cases (a).



**Fig. 3.** A typical random mesh generation.

Moreover, the elimination of close random circles can control the minimum distance between each stone aggregate and other ones. The amount of SA in CM,  $p$ , can be decreased by enlarging the minimum distances between RC's. Similarly, uniform aggregates can be reflected by constant radius RC's as in Figure 4-c.



**Fig. 4.** A typical models of random stone aggregates

### 3. Results

To meet the appropriate numerical solution accuracy, the produced numerical FEM results should be tested. The comparison of the numerical solution against close associative analytical solution is not available for this particular study. This is due to the complex geometry induced by random stone aggregate shapes and problem geometry. Alternatively, the variation of FEM solution with mesh refinement can be used to justify the numerical accuracy. For this study, the comparison of CM reaction forces associated with fine and coarse mesh is considered. Figure 5 shows a smaller

relative variation of reaction force with mesh refinement. The majority of cases have a relative error well below 2%. Therefore the results associated with fine mesh reflect adequate solution accuracy.

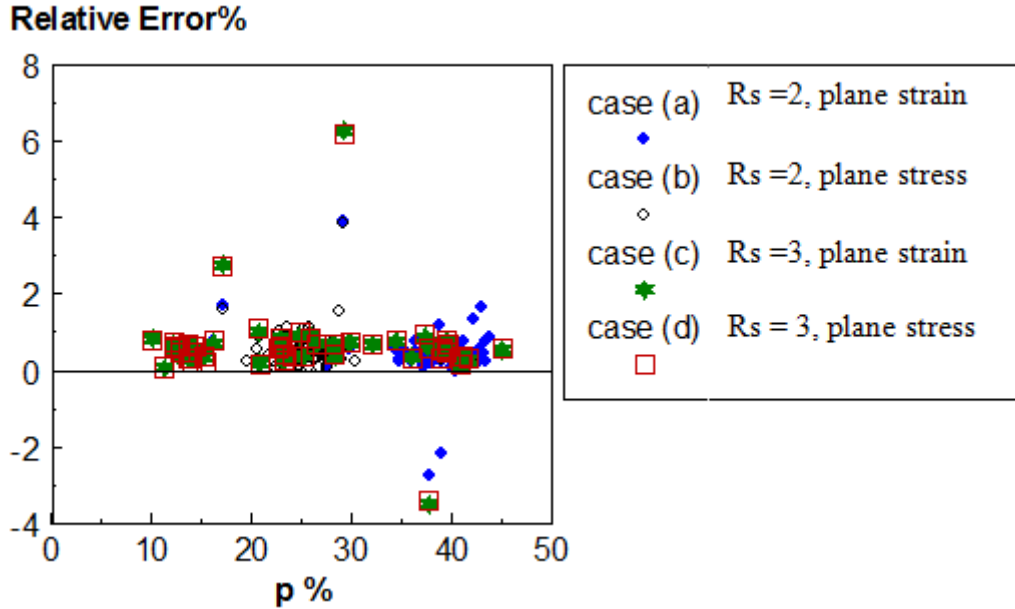


Fig. 5. Accuracy analysis with mesh refinement.

The magnitude of the modulus of elasticity is reflected by the compressive stiffness. Therefore, the results of compressive stiffness are compared with analytical bounds (rule of mixture) [21]. The rule of mixture represents the compressive stiffness under plane stress conditions as illustrated by Fig. 6. It is noted that the increase of SA amount in CM enlarges (to a limit) the compressive stiffness. Moreover, the increase of SA stiffness ( $R_s= 2$  to 3) results in a stiffer CM while all other parameters fixed. Notably, the relationship between the compressive stiffness of CM and  $p$  (plane stress), can be approximated as a non-linear curve. On the other hand, this curve has a concave nature, which is used to predict a lower stiffness of CM compared with that of a linear relationship. Thus care should be taken into consideration when seeking the stiffness of CM at an intermediate proportion of SA. The CM compressive strength may be expressed as a cubic polynomial of  $p$ . For  $R_s = 2$ ,  $E_{CM}$  (MPa) can be expressed as:

$$E_{CM} = 15 + 95 p + 0.2812 \times 10^{-3} p^2 + 0.2685 \times 10^{-5} p^3 \quad (2)$$

While for  $R_s =3$   $E_{CM}$  (MPa) can be expressed as:

$$E_{CM} = 15 + 132.2 p + 0.7701 \times 10^{-3} p^2 + 0.9073 \times 10^{-5} p^3 \quad (3)$$

It is noted that the change of  $E_{CM}$  is more rapid for  $R_s= 3$  than that of  $R_s= 2$  as indicated by both eq. 2 and 3. Similarly, the Poisson's ratio of CM,  $\nu_{CM}$ , has a non-linear association as in Figure 6-b. It is very clear that the predicted compressive stiffness agrees well with the rule of mixture bounds.



The compressive stiffness of CM under plane strain conditions are considered in Fig. 7. It is clearly shown that compressive stiffness associated with plane stress conditions is always less than plane strain conditions. This is anticipated as plane strain conditions introduce zero out of plane strain which in turn needs more compressive force to obtain the same deformation in other directions. In spite of the assumption of plane conditions of CM (and therefore 2-D conditions), the results showed good agreement with the rule mixture of 3-D conditions. However, to get more insight into a more realistic CM structure, 3-D conditions should be met by using 3-D FEM data. This is to be considered in the second part of this study.

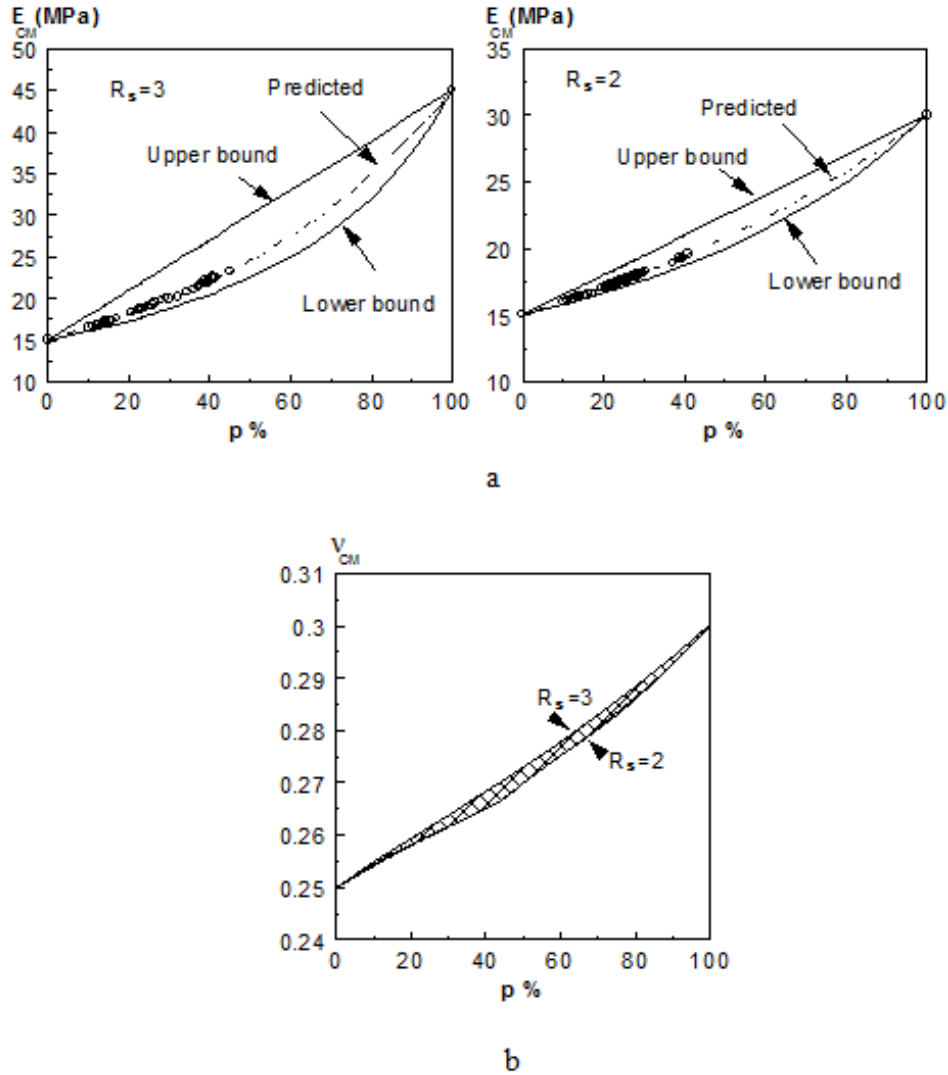


**Fig .6.** The variation of CM properties with p.

- a. ECM with P                      b.  $v_{CM}$  with p

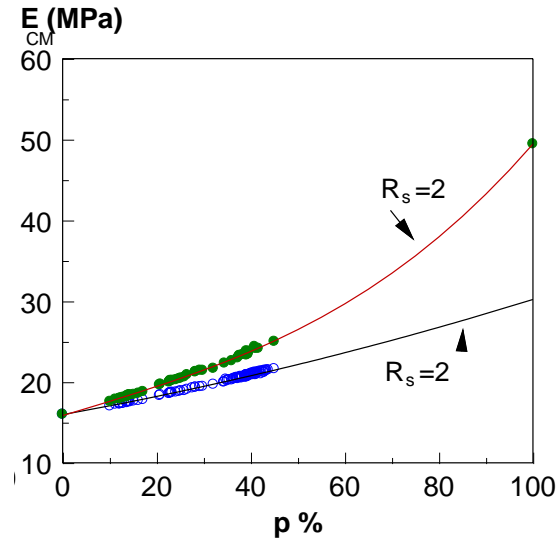


Fig. 7. The variation of CM properties with p.

## 4. Conclusion

A FEM input data for several case studies was developed and found useful and reliable in handling a variety of case studies. According to the results obtained, It is concluded that:

- for each case study, the input FEM data is adequate for problem modelling in terms of accuracy,
- the variation of the compressive stiffness of CM with the proportion of SA is non-linear and therefore care should be taken into consideration while using linear interpolation of CM properties,
- although the stone aggregates are assumed to be of cylindrical shapes (plane conditions), the compressive stiffness of CM agrees well with the rule of mixture.
- compressive stiffness associated with plane strain conditions is always more than that of plane stress conditions,
- the results associated with fine mesh reflect adequate solution accuracy.

## Acknowledgment

The ANSYS code is used in all calculations.

## References

- [1] B. Persson, "A comparison between mechanical properties of self-compacting concrete and the corresponding properties of normal concrete," *Cem. Concr. Res.*, vol. 31, no. 2, pp. 193–198, Feb. 2001.
- [2] A. Bahari, J. Berenjian, and A. Sadeghi-Nik, "Modification of Portland Cement with Nano SiC," *Proc. Natl. Acad. Sci. India Sect. A Phys. Sci.*, vol. 86, no. 3, pp. 323–331, Sep. 2016.

- [3] A. Sadeghi-Nik, J. Berenjian, A. Bahari, A. S. Safaei, and M. Dehestani, "Modification of microstructure and mechanical properties of cement by nanoparticles through a sustainable development approach," *Constr. Build. Mater.*, vol. 155, pp. 880–891, Nov. 2017.
- [4] A. Bahari, A. Sadeghi Nik, M. Roodbari, E. Mirshafiei, and B. Amiri, "Effect of Silicon Carbide Nano Dispersion on the Mechanical and Nano Structural Properties of Cement," *Natl. Acad. Sci. Lett.*, vol. 38, no. 4, pp. 361–364, Aug. 2015.
- [5] K.-R. Wu, B. Chen, W. Yao, and D. Zhang, "Effect of coarse aggregate type on mechanical properties of high-performance concrete," *Cem. Concr. Res.*, vol. 31, no. 10, pp. 1421–1425, Oct. 2001.
- [6] G. A. Rao and B. K. R. Prasad, "Influence of the roughness of aggregate surface on the interface bond strength," *Cem. Concr. Res.*, vol. 32, no. 2, pp. 253–257, Feb. 2002.
- [7] R. González-Peña, L. Martí-López, R. M. Cibrián-Ortiz de Anda, T. Molina-Jiménez, and C. Piqueres-Ayela, "Measurement of Young's modulus of cementitious materials using an electro-optic holographic technique," *Opt. Lasers Eng.*, vol. 36, no. 6, pp. 527–535, Dec. 2001.
- [8] D. L. Grote, S. W. Park, and M. Zhou, "Dynamic behavior of concrete at high strain rates and pressures: I. experimental characterization," *Int. J. Impact Eng.*, vol. 25, no. 9, pp. 869–886, Oct. 2001.
- [9] Y. L. Wong, L. Lam, C. S. Poon, and F. P. Zhou, "Properties of fly ash-modified cement mortar-aggregate interfaces," *Cem. Concr. Res.*, vol. 29, no. 12, pp. 1905–1913, Dec. 1999.
- [10] Z. M. Wang, A. K. H. Kwan, and H. C. Chan, "Mesoscopic study of concrete I: generation of random aggregate structure and finite element mesh," *Comput. Struct.*, vol. 70, no. 5, pp. 533–544, Mar. 1999.
- [11] K. Willam, I. Rhee, and G. Beylkin, "Multiresolution Analysis of Elastic Degradation in Heterogeneous Materials," *Meccanica*, vol. 36, no. 1, pp. 131–150, 2001.
- [12] S. Lai and M. Serra, "Concrete strength prediction by means of neural network," *Constr. Build. Mater.*, vol. 11, no. 2, pp. 93–98, Mar. 1997.
- [13] X.-H. Zhao and W. F. Chen, "Effective elastic moduli of concrete with interface layer," *Comput. Struct.*, vol. 66, no. 2–3, pp. 275–288, Jan. 1998.
- [14] Z. Hashin and P. J. M. Monteiro, "An inverse method to determine the elastic properties of the interphase between the aggregate and the cement paste," *Cem. Concr. Res.*, vol. 32, no. 8, pp. 1291–1300, Aug. 2002.
- [15] S. W. Park, Q. Xia, and M. Zhou, "Dynamic behavior of concrete at high strain rates and pressures: II. numerical simulation," *Int. J. Impact Eng.*, vol. 25, no. 9, pp. 887–910, Oct. 2001.
- [16] A. K. H. Kwan, Z. M. Wang, and H. C. Chan, "Mesoscopic study of concrete II: nonlinear finite element analysis," *Comput. Struct.*, vol. 70, no. 5, pp. 545–556, Mar. 1999.
- [17] G. Li, Y. Zhao, and S.-S. Pang, "A three-layer built-in analytical modeling of concrete," *Cem. Concr. Res.*, vol. 28, no. 7, pp. 1057–1070, Jul. 1998.
- [18] F. Khademi, S. M. Jamal, N. Deshpande, and S. Londhe, "Predicting strength of recycled aggregate concrete using Artificial Neural Network, Adaptive Neuro-Fuzzy Inference System and Multiple Linear Regression," *Int. J. Sustain. Built Environ.*, vol. 5, no. 2, pp. 355–369, Dec. 2016.
- [19] F. Khademi, M. Akbari, S. M. Jamal, and M. Nikoo, "Multiple linear regression, artificial neural network, and fuzzy logic prediction of 28 days compressive strength of concrete," *Front. Struct. Civ. Eng.*, vol. 11, no. 1, pp. 90–99, Mar. 2017.
- [20] A. P. (Arthur P. Boresi, K. P. (Ken P. Chong, and J. D. (James D. . Lee, *Elasticity in engineering mechanics*. Wiley, 2011.
- [21] W. D. Callister and D. G. Rethwisch, "Materials Science and Engineering An Introduction Library of Congress Cataloging-in-Publication Data," 2003.